iScience

CellPress
OPEN ACCESS

Article

Asperuloside Improves Obesity and Type 2 Diabetes through Modulation of Gut Microbiota and Metabolic Signaling

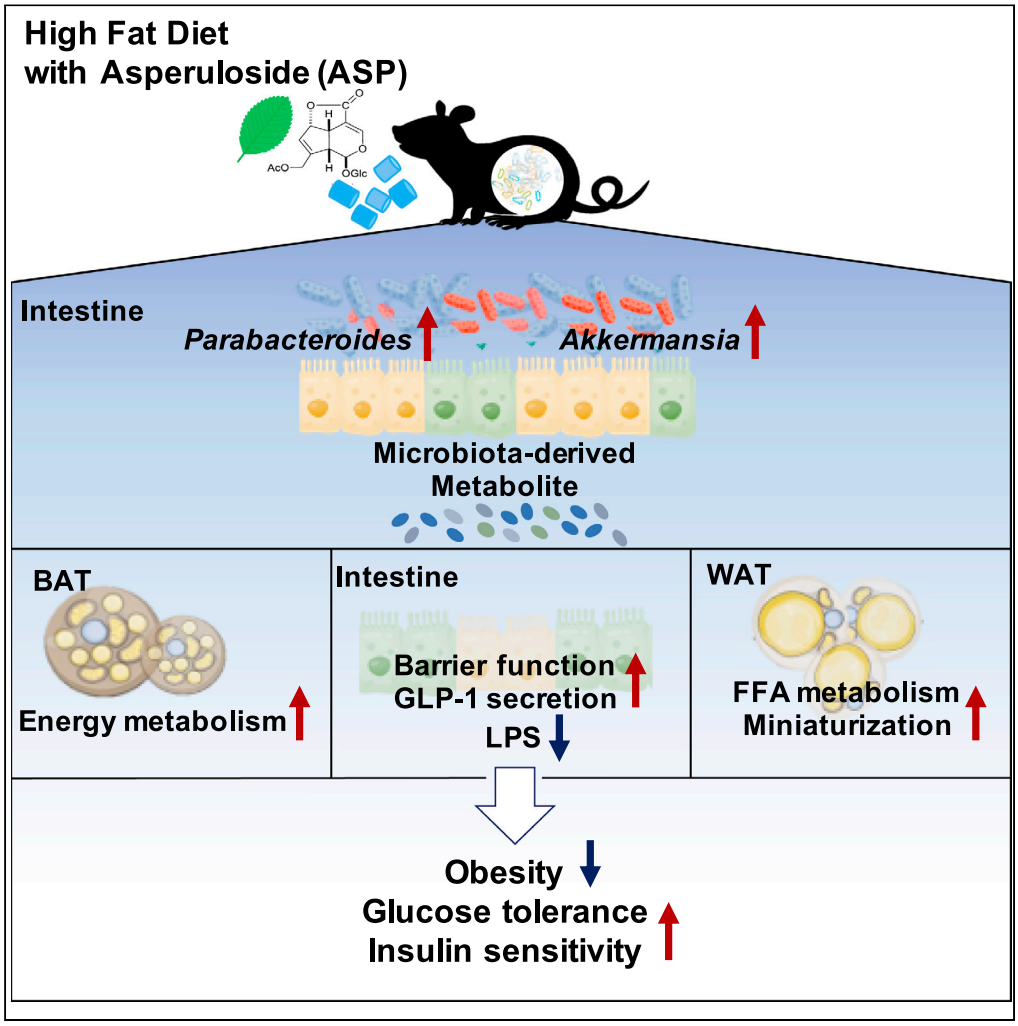

Anna Nakamura, Yoko Yokoyama, Kazuki Tanaka, ..., Johan Auwerx, Kazuo Tsubota, Mitsuhiro Watanabe

tsubota@z3.keio.jp (K.T.)
mitsuhiro.keio.hsl@gmail.com (M.W.)

HIGHLIGHTS

Asperuloside (ASP) treatment improved obesity-related metabolic dysfunction in mice

ASP administration changed intestinal metabolite via modulation of gut microbiota

ASP administration increased *Parabacteroides* and *Akkermansia* in intestine

Gut microbiota-derived metabolite improves adipose tissue and intestinal dysfunction

Nakamura et al., iScience *23*, 101522
September 25, 2020
https://doi.org/10.1016/j.isci.2020.101522

iScience

CellPress
OPEN ACCESS

Article

Asperuloside Improves Obesity and Type 2 Diabetes through Modulation of Gut Microbiota and Metabolic Signaling

Anna Nakamura,[1,2] Yoko Yokoyama,[1,2] Kazuki Tanaka,[1,3,4] Giorgia Benegiamo,[5] Akiyoshi Hirayama,[3] Qi Zhu,[2,6] Naho Kitamura,[1,2] Taichi Sugizaki,[7] Kohkichi Morimoto,[7] Hiroshi Itoh,[7] Shinji Fukuda,[3,4,8] Johan Auwerx,[5] Kazuo Tsubota,[2,9,*] and Mitsuhiro Watanabe[1,2,6,7,9,10,*]

SUMMARY

Asperuloside (ASP) is an iridoid glycoside that is extracted from *Eucommia* leaves. *Eucommia* is used in traditional Chinese medicine and has a long history of benefits on health and longevity. Here, we investigated the impact of ASP on obesity-related metabolic disorders and show that ASP reduces body weight gain, glucose intolerance, and insulin resistance effectively in mice fed with a high-fat diet (HFD). Intestinal dysbiosis is closely linked with metabolic disorders. Our data indicate that ASP achieves these benefits on metabolic homeostasis by reversing HFD-induced gut dysbiosis and by changing gut-derived secondary metabolites and metabolic signaling. Our results indicate that ASP may be used to regulate gut microbiota for the treatment of obesity and type 2 diabetes.

INTRODUCTION

Obesity has recently become epidemic, with one in three people being obese or overweight worldwide, and as such poses a major public health problem (Hoyt et al., 2014). Obesity has been linked to a variety of chronic diseases often within the context of the metabolic syndrome, a cluster of symptoms that include insulin resistance, type 2 diabetes, cardiovascular diseases, fatty liver, and even liver cancer (Osborn and Olefsky, 2012). According to recent data, extreme obesity could shorten the average life expectancy by about 14 years (Kitahara et al., 2014) and substances that prevent obesity could hence lead to the extension of a healthy lifespan.

Obesity results from the interaction of many genetic, metabolic, and environmental factors. In recent years, knowledge about the gut microbiota in health has grown tremendously (Cani and Delzenne, 2009). Intestinal bacteria contribute to the pathogenesis of obesity through a wide range of mechanisms that include, but are not restricted to, the promotion of energy absorption from diet, alterations in the production of intestinal hormones, and the induction of insulin resistance by obesity-induced inflammation (Bäckhed et al., 2007; Kimura et al., 2013; Ridaura et al., 2013). Antibiotics and prebiotics are being evaluated for the management of obesity and related metabolic disorders. Administration of antibiotics improves impaired glucose tolerance, and prebiotics reduce the influx of the endotoxin, lipopolysaccharide (LPS), by strengthening the barrier function of the intestinal tract. Antibiotics and prebiotics have also been reported to suppress and control obesity-induced inflammation (Cani et al., 2008, 2009). Also, recent studies revealed that some bacteria can change metabolic signaling pathways via their secondary metabolites. For example, in patients with type 2 diabetes, the intestinal bacteria composition and metabolites are different from those of healthy subjects (Sato et al., 2014). In addition, the presence of *Akkermansia* has been proposed to maintain gut health and glucose homeostasis, and recently, *Akkermansia* abundance has been linked with increased level of nicotinamide (Blacher et al., 2019). Also, *Parabacteroides* have been shown to attenuate obesity and metabolic dysfunctions via the production of succinate and secondary bile acids (Wang et al., 2019). Based on all these evidences, it is clear that change in the gut microbiota and their secondary metabolites are closely linked to the development of metabolic disease.

Asperuloside (ASP) is an iridoid glycoside derived from the leaves of the *Eucommia* tree (*Eucommia ulmoides Oliv.*). Its bark (Cortex Eucommiae) has been traditionally used in Chinese medicine for its analeptic, analgesic, sedative, antihypertensive, and diuretic properties. In recent years, *Eucommia* leaves have been shown to curb obesity (Hosoo et al., 2015), an effect that was linked to the main active compound, asperuloside (ASP) (Hirata et al., 2011). A previous study showed that administration of ASP

[1]Systems Biology Program, Graduate School of Media and Governance, Keio University, Fujisawa, Kanagawa 252-0882, Japan

[2]Health Science Laboratory, Keio Research Institute at SFC, Fujisawa, Kanagawa 252-0882, Japan

[3]Institute for Advanced Biosciences, Keio University, Tsuruoka, Yamagata 997-0052, Japan

[4]Intestinal Microbiota Project, Kanagawa Institute of Industrial Science and Technology, Kawasaki, Kanagawa 210-0821, Japan

[5]Laboratory of Integrative and Systems Physiology, École Polytechnique Fédérale de Lausanne (EPFL), Lausanne 1015, Switzerland

[6]Department of Environment and Information Studies, Keio University, Fujisawa, Kanagawa 252-0882, Japan

[7]Department of Internal Medicine, Keio University School of Medicine, Shinjuku, Tokyo 160-8582, Japan

[8]Transborder Medical Research Center, University of Tsukuba, Tsukuba, Ibaraki 305-8575, Japan

[9]Department of Ophthalmology, Keio University School of Medicine, Shinjuku, Tokyo 160-8582, Japan

[10]Lead Contact

*Correspondence: tsubota@z3.keio.jp (K.T.), mitsuhiro.keio.hsl@gmail.com (M.W.)

https://doi.org/10.1016/j.isci.2020.101522

reduced body weight gain by reducing visceral fat mass (Hirata et al., 2011). However, the underlying mechanism of how ASP affects weight gain and influences other obesity-related disorders remains unknown. Several compounds included in Chinese medicine are metabolized by gut bacteria into active intermediates (Lee et al., 2012). Here we report that ASP changes the gut microbiota composition and the production of secondary metabolites, affects whole-body signaling, and thereby curbs obesity and its related metabolic dysfunctions.

RESULTS

ASP Prevents High-Fat-Diet-Induced Obesity

First, we evaluated the metabolic phenotype of male mice fed normal chow (control), a high-fat diet (HFD), or a high-fat diet supplemented with ASP (HFD-Asp) for 12 weeks starting at the age of 5 weeks. When compared with animals fed chow, high-fat-fed animals gained significantly more weight. However, mice fed a HFD with ASP were resistant to body weight gain and their body weight remained similar to the control group (Figure 1A). There was no significant difference between the energy intakes of HFD- and ASP-treated mice (Figure 1A). In addition, liver, epididymal white adipose tissue (epiWAT), and mesenteric WAT (mWAT) mass were all decreased in ASP-treated mice (Figure 1B). Furthermore, serum triglycerides (TG) were significantly lower and total cholesterol levels tended to decrease in ASP-treated animals, whereas free fatty acid levels were similar in the ASP and HFD treatment groups (Figure 1C). These results suggest that ASP reduces body weight gain and fat accumulation, as well as serum lipid parameters induced by HFD.

ASP Improves Glucose Homeostasis and Insulin Resistance

Glucose metabolism is often abnormal in obese patients. Given the robust impact of ASP on body weight gain, we next investigated the effect of ASP on glucose metabolism. The administration of ASP improves glucose clearance during an oral glucose tolerance test (OGTT) (Figure 1D). The lower plasma insulin levels during OGTT indicated that increased insulin sensitivity led to improved glucose metabolism in ASP-treated mice (Figure 1E). Interestingly, the levels of active GLP-1, an incretin secreted from the gut L-cells upon feeding and that induces insulin secretion, was increased in ASP-treated mice (Figure 1F). Furthermore, intraperitoneal insulin tolerance test (IPITT) showed that mice fed HFD became insulin resistant, whereas ASP significantly improved insulin sensitivity (Figure 1G). Taken together, ASP improves glucose tolerance and insulin sensitivity and increases GLP-1 levels. We next tested whether ASP may have a direct effect to stimulate GLP-1 release from intestinal L-cells. We therefore incubated NCI-H716 cells, which secrete GLP-1 (Reimer et al., 2001), with ASP for 30 min and 6 h. As positive control we used the bile acid taurocholic acid (TCA). TCA stimulated GLP-1 secretion both after 30-min and 6-h exposures, whereas we did not observe an increase in GLP-1 concentration when cells were treated with ASP (Figures 1H and S1). This result indicated that the observed effect of ASP on GLP-1 secretion *in vivo* is indirect.

ASP Reverses High-Fat-Diet-Induced Gut Dysbiosis

Given the importance of the gut microbiome in metabolic homeostasis (Cani and Delzenne, 2009), we next performed bacterial 16S rRNA gene sequencing of cecal samples. First, we evaluated the groups fed with control, HFD, and HFD-ASP diets for changes in the microbiome at the phylum level. UniFrac-based principal coordinates analysis revealed a distinct clustering of the microbiota composition for each treatment group (Figure 2A). Hierarchical clustering at the phylum level showed that the microbial communities in the cecum of the ASP-fed mice were significantly different from those of the control and HFD-fed mice; ASP treatment increased Bacteroidetes and Verrucomicrobia (Figure 2B). Also, the ratio of Bacteroidetes/Firmicutes was increased in the HFD-Asp group (Figure 2C). To access specific changes in microbiota, we analyzed the relative abundance of the predominant taxa identified from sequencing in the three diet groups. Phylum-level changes further confirmed a higher level of Bacteroidetes to Firmicutes in mice that received ASP supplementation (Figure 2D). In genus-level analysis, ASP increased *Bacteroides* and *Parabacteroides* (Figure S2A).

ASP Increases Beneficial Gut Bacteria in an HFD-Fed Mouse Model

We next investigated, which specific bacteria at the genus level were increased by ASP supplementation. Community structure analysis using correlation analysis at the genus level in HFD versus HFD-Asp group showed that ASP supplementation correlated positively with *Akkermansia*, *Parabacteroides, Bacteroides, Sutterella, Anaerostipes, Roseburia,* and *Coprobacillus* abundance (Figure S2B). Also, linear discriminant analysis effect size analysis shows a similar pattern as that seen in the correlation analysis (Figure 2E).

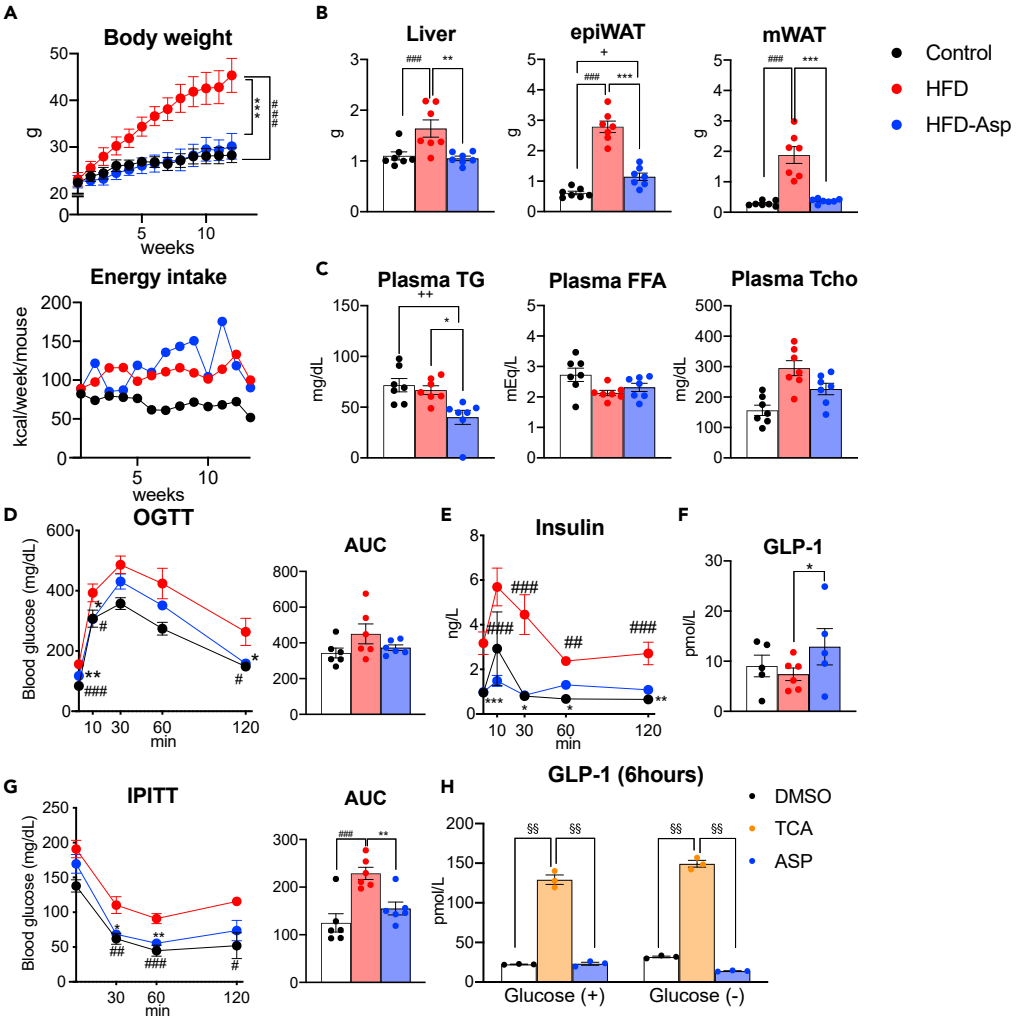

Figure 1. ASP Prevents High-Fat Diet-Induced Obesity and Improves Glucose Tolerance and Insulin Resistance

(A–G) Male C57BL/6J mice aged 5 weeks were fed with a control diet (10% kcal fat; Control), a high-fat diet (60% kcal fat; HFD), or a high-fat diet supplemented with 0.25% w/w asperuloside (HFD-Asp) for 12 weeks (n = 5-7 for each group). (A) Body weight evolution and food intake of C57BL/6J mice in the different diet groups. Energy intake was measured as the average food intake per mouse in a week. (B) Comparison of liver, mWAT, and epiWAT tissue weights after 12 weeks of treatment with different diets. (C) Plasma total cholesterol (Tcho), triglyceride (TG), and free fatty acid (FFA) levels after 12 weeks of ASP supplementation. (D) Serum glucose levels and AUC during OGTT. (E) Plasma insulin concentration during OGTT. (F) Plasma active GLP-1 levels 10 min after administration of glucose during the OGTT. (G) The reduction of serum glucose levels and AUC during IPITT.

(H) GLP-1 concentration secreted from NCI-H716 cell line cultured for 6 h.

(A–G) Results are expressed as mean ± SEM (n = 5–7 mice for each group). *p < 0.05, **p < 0.01, ***p < 0.001 HFD versus HFD-Asp, #p < 0.05, ##p < 0.01, ###p < 0.001 HFD versus Control, +p < 0.05, ++p < 0.01, +++p < 0.001 Control versus HFD-Asp. Statistical analysis with one-way ANOVA followed by Tukey's multiple comparison test or Dunnett's multiple comparison test. (H) Results are expressed as mean ± SEM. §p < 0.05, §§ <0.01, versus TCA treatment. Statistical analysis with one-way ANOVA followed by Dunnett's multiple comparison test. See also Figure S1.

We next measured the relative abundance of four bacteria, i.e., *Akkermansia*, *Roseburia*, *Anaerostipes*, and *Parabacteroides*; ASP increases the actual abundance of all four bacteria (Figure 2F). *Akkermansia* has been reported to strengthen intestinal tight junctions and control the inflow of LPS into the blood (Everard et al., 2013). *Roseburia* and *Anaerostipes* produce short-chain fatty acids (SCFAs) via metabolization of carbohydrate (Basson et al., 2016), and *Parabacteroides* are known to improve glucose homeostasis by producing succinate (Wang et al., 2019). These results show that ASP changes the microbial community and increases the number of bacteria with a positive health impact.

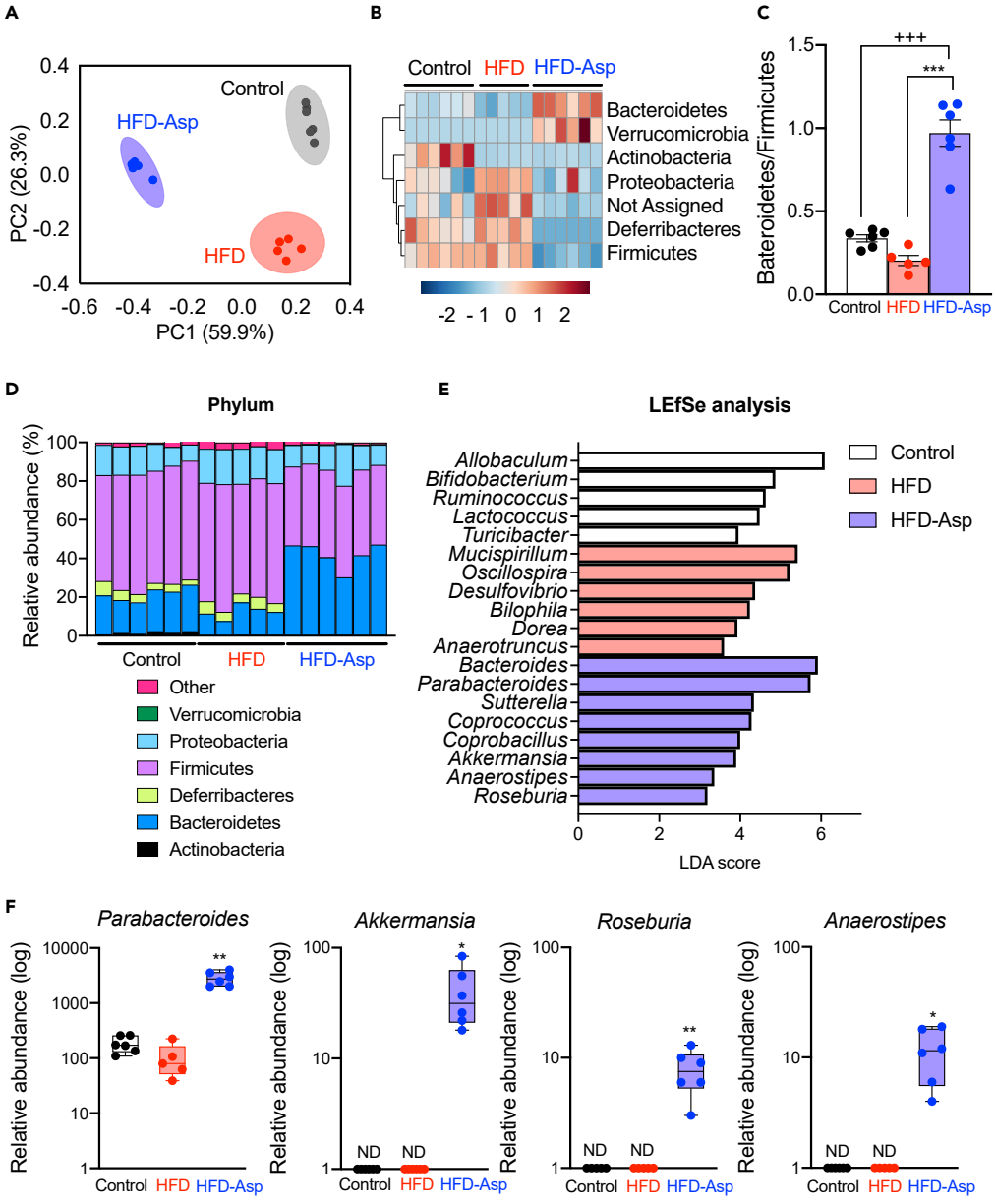

Figure 2. ASP Modulates the Composition of Gut Microbiota Community

(A–F) Analysis of the 16S rRNA gene sequences of cecal contents of the mice used in Figure 1. (A) Principal coordinates analysis of the 16S rRNA data. (B) Heatmap of the microbiota components at the class level. (C) The ratio of Bacteroidetes/Firmicutes. (D) Phylum-level taxonomic distributions of the microbial communities in cecal contents of mice fed with the three different diets. (E) Linear discriminant analysis effect size (LEfSe) analysis. (F) Relative abundance of four prototypical bacteria at the genus level.

Results are expressed as mean ± SEM (n = 5–6 mice for each group). *p < 0.05, **p < 0.01, ***p < 0.001 HFD versus HFD-Asp; #p < 0.05, ##p < 0.01, ###p < 0.001 HFD versus Control; +p < 0.05, ++p < 0.01, +++p < 0.001 Control versus HFD-Asp. See also Figure S2.

ASP Alters Whole-Body Metabolism by Changing Cecal Metabolite Levels

Given the important changes in the intestinal microbiome analysis, we next measured changes in the metabolome induced by ASP in the cecal content using Capillary electrophoresis with electrospray ionization time-of-flight mass spectrometry (CE-TOFMS). Principal-component analysis of the cecal metabolites showed a clear separation among three diets in the first component (Figure 3A). In mice receiving ASP

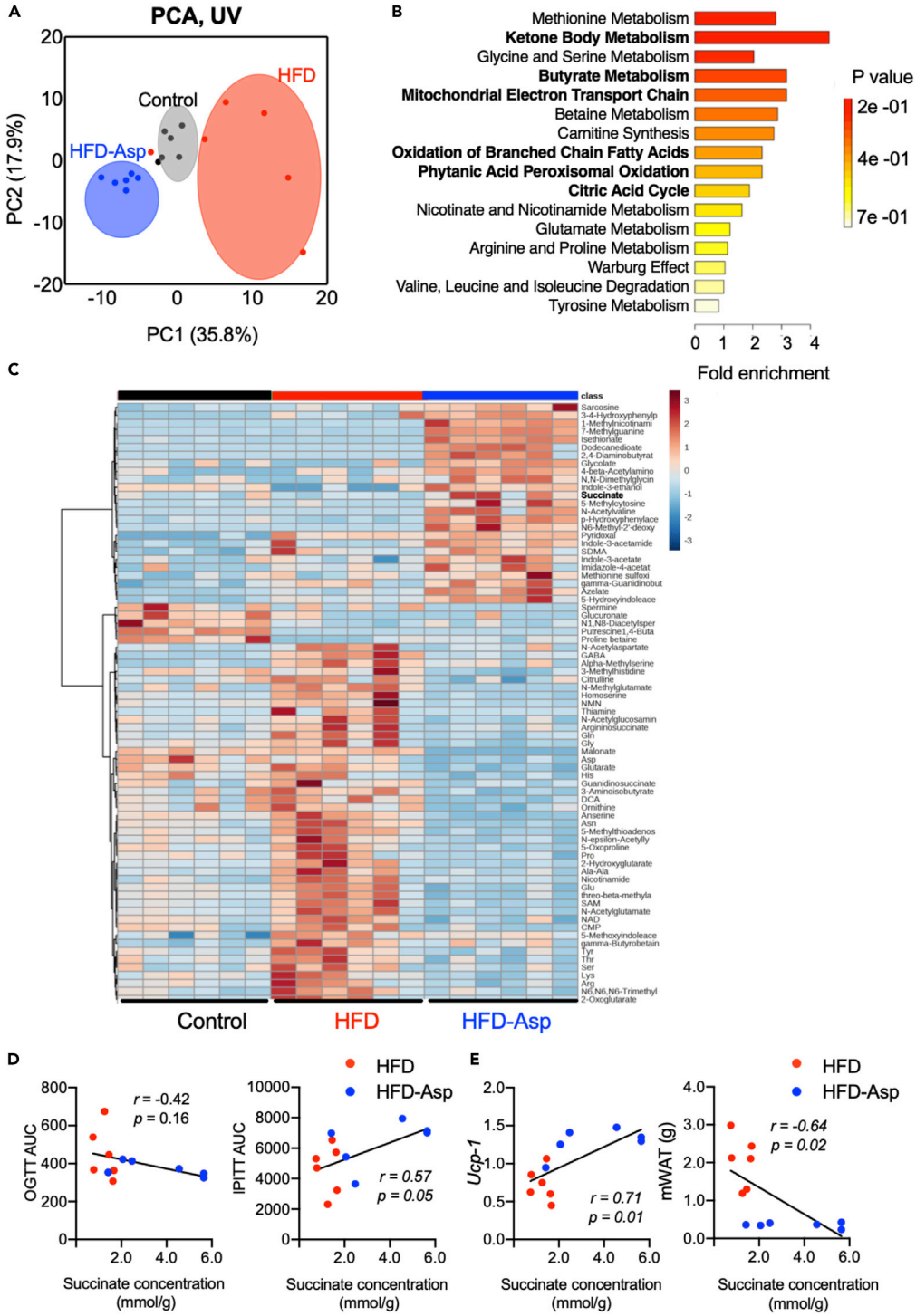

Figure 3. ASP Remodeling of the Cecal Metabolite Profile and Increase in Succinate Concentration

(A–E) Cecal metabolome analysis on the mice used in Figure 1. (A) Principal-component analysis (PCA) of the cecal metabolome profiles normalized by unit valiance (UV). (B) Enrichment analysis of cecal metabolites that were changed by more than 2-fold between HFD after ASP supplementation. Bold character shows related to lipid metabolism. (C) Heatmap showing the concentrations of the top 75 metabolites that were quantified. (D) Correlation analysis between succinate concentration and glucose tolerance and insulin sensitivity. (E) Correlation analysis between succinate concentration and *Ucp-1* expression in brown adipose tissue (BAT) and mesenteric white adipose tissue (mWAT) weight.

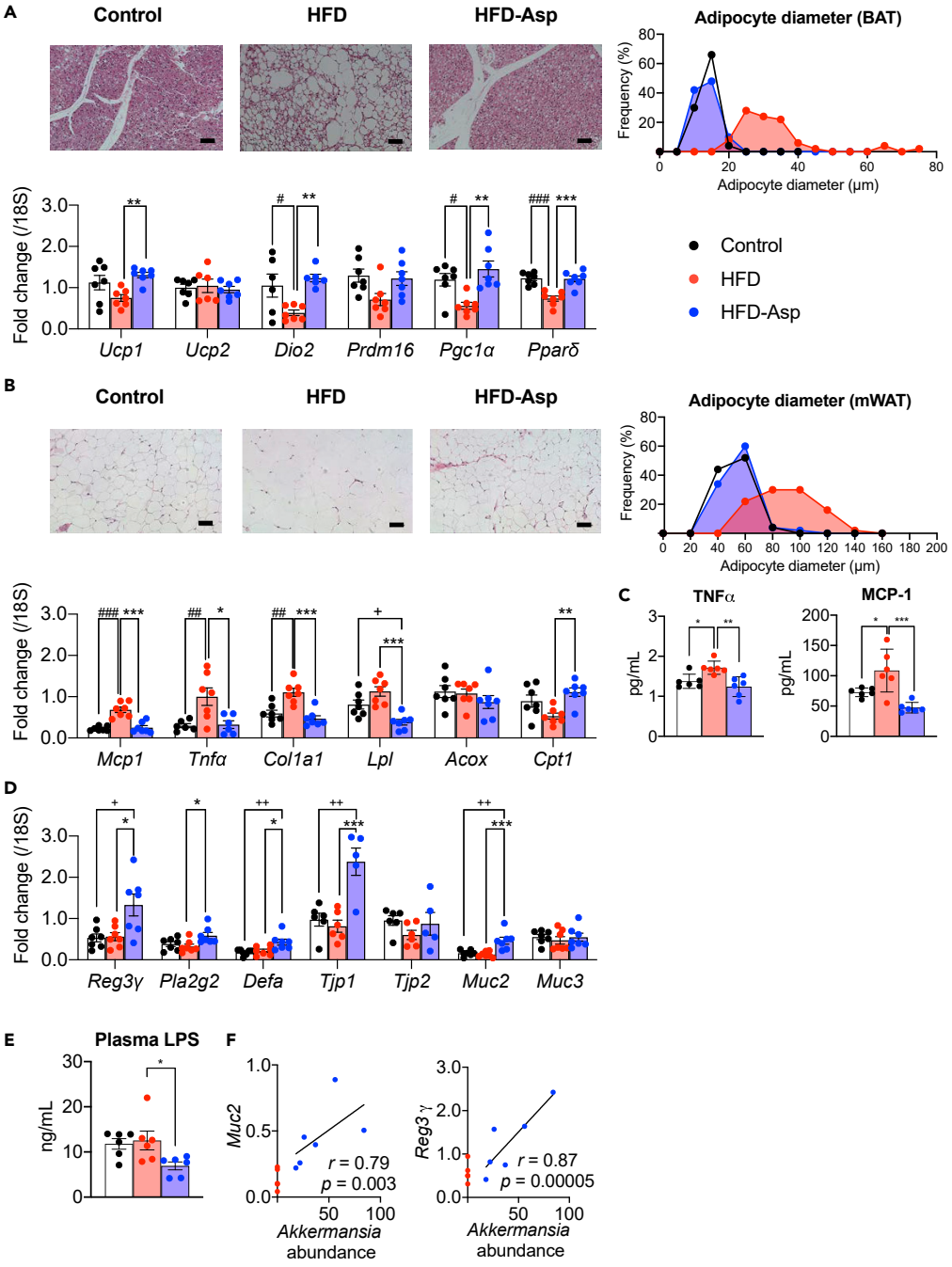

Figure 4. Impact of ASP on Several Organs

(A–E) Histological analysis, LPS measurement, and qPCR analysis on the mice used in Figure 1. (A) Histological analysis and expression of mRNA levels of selected genes; qPCR analysis in the brown adipocyte. Brown adipocyte morphology was assessed by H&E staining (scale bar, 50 μm). (B) Histological analysis and expression of mRNA levels of selected genes; qPCR analysis in the mesenteric white adipose tissue (mWAT). Morphology of mWAT was assessed by H&E staining (scale bar, 50 μm). (C) Plasma level of TNFα and MCP-1 analysis measured by ELISA. (D) qPCR analysis in ileum. (E) Plasma LPS concentration.

(F) Correlation analysis between *Muc2* and *Reg3γ* expression and *Akkermansia* abundance. y axis: expression of *Muc2* and *Reg3γ*; x axis: *Akkermansia* abundance of cecal contents. The intestinal portions are collected from a section 3 cm above the cecum.

Figure 4. *Continued*

Results are expressed as mean ± SEM (n = 5–7 mice for each group). *p < 0.05, **p < 0.01, ***p < 0.001 HFD versus HFD-Asp; #p < 0.05, ##p < 0.01, ###p < 0.001 HFD versus Control; +p < 0.05, ++p < 0.01, +++p < 0.001 Control versus HFD-Asp. Statistical analysis with one-way ANOVA followed Tukey's multiple comparison test. See also Figure S3 and Table S1.

in the diet the most changed cecal metabolites were related to the metabolism of ketone bodies, butyrate, and other fatty acids (Figure 3B). These results indicate that ASP may mainly affect lipid metabolism. The hierarchical clustering of detected features showed qualitative differences between the HFD and HFD-Asp groups (Figure 3C). In HFD, the levels of glycine, L-glutamic acid, and other amino acid-derived compounds increased. In HFD-Asp, the levels of sarcosine and dimethylglycine (involved in methionine metabolism) and succinate (a metabolite from the TCA cycle, ketone body metabolism, and other lipid metabolism pathway) increased (Figure 3C). Considering the result from the enrichment analysis (Figure 3B), we focused on the lipid metabolite succinate. Succinate, which is detected in HFD-Asp group, is the precursor of SCFAs. In addition, succinate is produced by gut microbiota *Parabacteroides*, which have increased significantly in HFD-Asp mice. It is known to improve glucose intolerance and insulin resistance (De Vadder et al., 2016). In our study, succinate was negatively correlated with the area under the curve (AUC) during OGTT and was positively correlated with the drop rate in glucose during IPITT (AUC below baseline), which are indicators of glucose intolerance and insulin sensitivity, respectively (Figure 3D). From the result of enrichment analysis, we focused on the relationship between adipocyte metabolism and succinate. Recent study reported that the accumulation of succinate activates brown adipose tissue (BAT) thermogenesis (Mills et al., 2018), we also confirmed a positive correlation between *Ucp-1* expression which high expression in BAT and succinate concentration in our study (Figure 3E). Furthermore, there are negative correlations with the weight of each white adipose tissue (WAT) depot and succinate levels (Figures 3E and S3B).

ASP Improves Adipose Tissue Metabolism

Obesity is typified by TG accumulation in adipocytes, which become enlarged and hypertrophic. Bloated fat cells secrete tumor necrosis factor alpha (TNF-α) and resistin, which are mediators of insulin resistance (Hotamisligil, 1999) that are closely linked to type 2 diabetes. A recent study reported that SCFAs often derived from gut metabolites suppress fat accumulation (Kimura et al., 2013). As ASP administration attenuated the increase in mWAT and epiWAT weight induced by HFD (Figure 1B), we investigated whether adipose tissue morphology and gene expression patterns were changed by ASP. On histopathologic examination, adipocytes in the mWAT, epiWAT, and BAT were hypertrophic in HFD-fed mice, an effect that was completely prevented by ASP (Figures 4A, 4B, and S3A). The adipocyte diameter was decreased in mWAT, epiWAT, and BAT (Figures 4A, 4B, and S3A). In BAT, transcript levels of *Ucp1,* which uncouples oxidative phosphorylation and utilizes β-oxidation of fatty acids released from triacylglycerol, were remarkably induced in the ASP group. Furthermore, transcript levels of *Dio2* and *Pgc1α* increased by ASP treatment; *Dio2* and *Pgc1α* are two principal players that facilitate the induction of genes involved in BAT thermogenesis. Also, mRNA levels of *Pparδd* were markedly increased in the ASP group (Figure 4A); the PPAR family of nuclear receptors is the main regulator of fatty acid β-oxidation and energy homeostasis in mitochondria. These data support the fact that ASP induces the miniaturization at the histological level in BAT.

In WAT, mRNA levels of tumor necrosis factor alpha (*Tnfα*) and of monocyte chemoattractant protein 1 (*Mcp1*) that regulate migration and infiltration of monocytes/macrophages were reduced by ASP. Also, the plasma protein level of TNFα and MCP-1 were decreased in accordance with results of relative mRNA expressions (Figure 4C). Furthermore, the mRNA level of the fibrosis marker, collagen type 1 alpha1 (*Col1a1*), was decreased upon ASP treatment. In addition, the transcripts coding for the lipolytic enzyme lipoprotein lipase (*Lpl*) and carnitine palmitoyl transferase 1 (*Cpt1*) were significantly increased after ASP treatment (Figures 4B and S3A). Of note is the fact that transcript levels were altered similarly in both mWAT and epiWAT.

ASP Improves Intestinal Barrier Function

It has been reported that obesity is accompanied by a compromised intestinal barrier function, which in turn is involved in the development of insulin resistance and impaired glucose tolerance (Monk et al., 2019). In our study of the gut microbial structural community, *Akkermansia* was increased in ASP-supplemented mice. The presence of *Akkermansia* is associated with improved metabolic control and a reduction of inflammation (Anhê et al., 2015). According to microbiome analysis, we investigated intestinal barrier

function. In qPCR analysis, transcript levels of the anti-bacterial peptides (*Reg3γ*, *Pla2g2*, *Defa*); of markers of the intestinal mucous layer (*Muc2*, *Muc3*), which protect the epithelium against noxious agents, viruses, and pathogenic bacteria (Hartmann et al., 2016); and of players in tight junctions (*Tjp1*, *Tjp2*) are induced in the ASP supplementation group (Figure 4D). Furthermore, plasma LPS concentration was decreased in ASP-supplemented group (Figure 4E). These findings hence suggest that ASP improves intestinal barrier function, which was corroborated by the tight positive correlation between *Akkermansia* abundance and expression of *Muc2* and *Reg3γ* (Figure 4F).

DISCUSSION

Our study addressed the mechanism of how ASP, the active ingredient of *Eucommia* leaf, improves metabolic health. Our findings revealed that changes in the gut microbiota community are an important aspect involved in the efficacy of ASP to improve obesity and associated phenotypes, such as insulin resistance and glucose intolerance.

ASP changes the gut microbiota at the phylum level with an important impact on the ratio of Bacteroidetes/Firmicutes. Previous studies suggested that microbiota in obese mice are enriched in Firmicutes and decreased in Bacteroides (Ridaura et al., 2013), an effect that we also observed in our HFD-fed mice. Importantly, ASP administration decreased the amount of Firmicutes and increased that of Bacteroidetes.

Also, at the genus level, ASP induced changes and increased the amounts of *Parabacteroides*. *Parabacteroides*, one of the 18 core members in the human gut microbiota (Falony et al., 2016), plays important functions in modulating host metabolism (Wang et al., 2019). These findings suggest that gut microbiota is an important target for both prevention and therapeutics of obesity and metabolic dysfunctions. A recent study reported that *Parabacteroides* produces succinate, and succinate supplementation in the diet was shown to decrease hyperglycemia in *Ob/Ob* mice via the activation of intestinal gluconeogenesis (IGN) (Wang et al., 2019). Succinate-activated IGN suppressed hepatic glucose production by decreasing the activity of G6Pase and by increasing the glucose-6-phosphate (Glu6P) content in the liver to modulate glucose homeostasis. Our study also confirmed increased succinate levels in the cecal contents of the ASP-treated mice, suggesting that ASP supplementation may modulate glucose homeostasis through *Parabacteroides*-derived succinate.

Parabacteroides, *Roseburia*, and *Anaerostipes* produce SCFA and were significantly increased by ASP treatment. SCFAs are important secondary metabolites that activate certain G protein-coupled receptors (GPCRs) and as such improve metabolite signaling (Kimura et al., 2013). We found that the active GLP-1 concentration was higher in the ASP-treated animals than in HFD groups. GLP-1 is an incretin, which stimulates insulin secretion from pancreatic β-cell in a glucose-dependent fashion (Doyle and Egan, 2007), and increasing and stabilizing GLP-1 levels is an important strategy to manage type 2 diabetes (Nauck et al., 2011). The changes in GLP-1 levels induced by ASP can be explained by alterations in the gut microbiota and their subsequent impact on secondary metabolites. Recently, SCFAs were shown to activate the gut receptors, GPR41/43, and as such stimulate L-cells to release GLP-1. We observed that propionate and a precursor of SCFAs, succinate, were increased by ASP treatment in the cecum, consistent with the enrichment of SCFA-producing bacteria. These findings suggest that ASP may favor GLP-1 secretion by the activation of specific GPCR signaling cascades in colonic L-cells by increasing SCFA-producing bacteria. Furthermore, GPR43 activation by SCFA suppresses insulin-mediated fat accumulation (Kimura et al., 2013); this mechanism may mediate the reduction in mWAT and epiWAT hypertrophy in the ASP groups. Our *in vitro* data showing the absence of a direct effect of ASP on GLP-1 release in cultured NCI-H716 L-cells are consistent with such an indirect effect mediated by the increase in SCFA levels (Figures 1H and S1).

In addition, we found that *Akkermansia muciniphila* is robustly increased in ASP-treated mice. In type 2 diabetes, *Akkermansia* have been closely linked to the attenuation of insulin resistance and obesity (Everard et al., 2011), and a recent clinical study showed that *Akkermansia* supplementation improves obesity (Depommier et al., 2019). It has been reported that the increase in *Akkermansia* suppressed intestinal inflammation, strengthens the barrier function of the intestinal epithelium, suppresses the inflow of LPS, and prevents the development of liver steatosis, insulin resistance, and type 2 diabetes (Cani and de Vos, 2017). Our study shows that *Akkermansia* was robustly induced in the HFD-Asp group. Improved metabolic dysfunctions could be explained by the induction of *Akkermansia*. Furthermore, the changes in gene expression observed in the intestine would support such a hypothesis as transcripts of *Muc2*,

the predominant secreted mucin from the ileum and colon, were increased (Velcich et al., 2002), and *Muc2* deficiency in mice is associated with disruption of epithelial homeostasis and the development of colon cancer (Hsu et al., 2017). In combination, our results suggest that ASP has a major role on the gut microbiome, not only altering the production of metabolites with signaling and energetic functions but also potentially strengthening gut barrier function.

In conclusion, our study suggests that ASP is an interesting naturally derived compound that through pleiotropic changes in the gut microbiota and an impact on intestinal barrier function and metabolite production can improve obesity and associated metabolic dysfunction.

Limitations of the Study

In this study, we revealed that ASP changes gut microbiota composition and increases some beneficial bacteria. However, the detailed mechanism of how ASP affects gut microbiota is unknown. Further study is needed to confirm whether ASP acts like prebiotics and has antibacterial activity. In addition, future studies such as fecal transplantation are needed to strengthen our hypothesis that gut microbiota is beneficial for HFD-Asp-fed mice. Our study shows the effect of BAT by ASP. However, the actual energy expenditure and the beneficial effect of ASP under thermoneutrality are still to be determined.

Resource Availability

Lead Contact

Further information and requests for resources should be directed to and will be fulfilled by the Lead Contact, Mitsuhiro Watanabe (mitsuhiro.keio.hsl@gmail.com).

Materials Availability

This study did not generate new unique reagents.

Data and Code Availability

Microbiome sequencing data have been deposited at the DDBJ Sequence Read Archive (http://trace.ddbj.nig.ac.jp/dra/) under accession number DRA009825.

METHODS

All methods can be found in the accompanying Transparent Methods supplemental file.

SUPPLEMENTAL INFORMATION

Supplemental Information can be found online at https://doi.org/10.1016/j.isci.2020.101522.

ACKNOWLEDGMENTS

We thank Dr. Setsuo Takekawa at Shonan Keiiku Hospital and Dr. Masaru Tomita at Institute for Advanced Biosciences (IAB), Keio University for providing continuous support. We also thank Dr. Tetsuya Hirata, Yoko Takashina, Dr. Sansho Nishibe and Dr. Aw Wanping for helpful discussion. We would like to thank Yuka Ohara and Mitsuko Komatsu and Dr. Chiharu Ishii for providing technical support for metabolome and microbiome analysis. In addition, we would like to express our gratitude to Narumi Hanazato and Naoya Nakagawa for their continuous support. This study was supported in part by JSPS KAKENHI (JP16H05292 to M.W.; JP19K11751 to Y.Y.), Taikichiro Mori Memorial Research Grants (to A.N.), the Ryoichi Sasakawa Young Leaders Fellowship Fund (to A.N.), JSPS KAKENHI (18H04805 to S.F.), JST PRESTO (JPMJPR1537 to S.F.), AMED-CREST (JP19gm1010009 to S.F.), JST ERATO (JPMJER1902 to S.F.), the Takeda Science Foundation (to S.F.), the Food Science Institute Foundation (to S.F.), and the Program for the Advancement of Research in Core Projects under Keio University's Longevity Initiative (to S.F., H.I., K.Tsubota, and M.W.). The work in J.A. laboratory was supported by grants from Ecole Polytechnique Federale de Lausanne (EPFL), the European Research Council (ERC-AdG-787702 to J.A.), and the Swiss National Science Foundation (SNSF 31003A_179435 to J.A.).

AUTHOR CONTRIBUTIONS

The study was conceived and designed by A.N. and M.W. A.N., Y.Y., K.Tanaka, G.B., Q.Z., N.K., T.S. and K.M. performed experiments. K.Tanaka, A.H. and S.F. conducted microbiome and metabolome analyses.

A.N., G.B., H.I., M.W. and J.A. wrote the manuscript, and all authors gave critical comments on it. K.Tsubota. and M.W. are the guarantors of this study and, as such, had complete access to all study data and take responsibility for the integrity of the data and accuracy of the data analysis.

DECLARATION OF INTERESTS

The authors declare no competing interests.

Received: May 20, 2020
Revised: June 5, 2020
Accepted: August 28, 2020
Published: September 25, 2020

REFERENCES

Anhê, F.F., Roy, D., Pilon, G., Dudonné, S., Matamoros, S., Varin, T.V., Garofalo, C., Moine, Q., Desjardins, Y., Levy, E., et al. (2015). A polyphenol-rich cranberry extract protects from diet-induced obesity, insulin resistance and intestinal inflammation in association with increased Akkermansia spp. population in the gut microbiota of mice. Gut *64*, 872–883.

Bäckhed, F., Manchester, J.K., Semenkovich, C.F., and Gordon, J.I. (2007). Mechanisms underlying the resistance to diet-induced obesity in germ-free mice. Proc. Natl. Acad. Sci. U S A *104*, 979–984.

Basson, A., Trotter, A., Rodriguez-Palacios, A., and Cominelli, F. (2016). Mucosal interactions between genetics, diet, and microbiome in inflammatory bowel disease. Front. Immunol. *7*, 290.

Blacher, E., Bashiardes, S., Shapiro, H., Rothschild, D., Mor, U., Dori-Bachash, M., Kleimeyer, C., Moresi, C., Harnik, Y., Zur, M., et al. (2019). Potential roles of gut microbiome and metabolites in modulating ALS in mice. Nature *572*, 474–480.

Cani, P.D., and Delzenne, N. (2009). The role of the gut microbiota in energy metabolism and metabolic disease. Curr. Pharm. Des. *15*, 1546–1558.

Cani, P.D., and de Vos, W.M. (2017). Next-generation beneficial microbes: the case of Akkermansia muciniphila. Front. Microbiol. *8*, 1765.

Cani, P.D., Bibiloni, R., Knauf, C., Waget, A., Neyrinck, A.M., Delzenne, N.M., and Burcelin, R. (2008). Changes in gut microbiota control metabolic endotoxemia-induced inflammation in high-fat diet-induced obesity and diabetes in mice. Diabetes *57*, 1470–1481.

Cani, P.D., Possemiers, S., Van de Wiele, T., Guiot, Y., Everard, A., Rottier, O., Geurts, L., Naslain, D., Neyrinck, A., Lambert, D.M., et al. (2009). Changes in gut microbiota control inflammation in obese mice through a mechanism involving GLP-2-driven improvement of gut permeability. Gut *58*, 1091–1103.

Depommier, C., Everard, A., Druart, C., Plovier, H., Van Hul, M., Vieira-Silva, S., Falony, G., Raes, J., Maiter, D., Delzenne, N.M., et al. (2019). Supplementation with Akkermansia muciniphila in overweight and obese human volunteers: a proof-of-concept exploratory study. Nat. Med. *25*, 1096–1103.

Doyle, M.E., and Egan, J.M. (2007). Mechanisms of action of glucagon-like peptide 1 in the pancreas. Pharmacol. Ther. *113*, 546–593.

Everard, A., Lazarevic, V., Derrien, M., Girard, M., Muccioli, G.G., Neyrinck, A.M., Possemiers, S., Van Holle, A., François, P., de Vos, W.M., et al. (2011). Responses of gut microbiota and glucose and lipid metabolism to prebiotics in genetic obese and diet-induced leptin-resistant mice. Diabetes *60*, 2775–2786.

Everard, A., Belzer, C., Geurts, L., Ouwerkerk, J.P., Druart, C., Bindels, L.B., Guiot, Y., Derrien, M., Muccioli, G.G., Delzenne, N.M., et al. (2013). Cross-talk between Akkermansia muciniphila and intestinal epithelium controls diet-induced obesity. Proc. Natl. Acad. Sci. U S A *110*, 9066–9071.

Falony, G., Joossens, M., Vieira-Silva, S., Wang, J., Darzi, Y., Faust, K., Kurilshikov, A., Bonder, M.J., Valles-Colomer, M., Vandeputte, D., et al. (2016). Population-level analysis of gut microbiome variation. Science *352*, 560–564.

Hartmann, P., Seebauer, C.T., Mazagova, M., Horvath, A., Wang, L., Llorente, C., Varki, N.M., Brandl, K., Ho, S.B., and Schnabl, B. (2016). Deficiency of intestinal mucin-2 protects mice from diet-induced fatty liver disease and obesity. Am. J. Physiol. Gastrointest. Liver Physiol. *310*, 310–322.

Hirata, T., Kobayashi, T., Wada, A., Ueda, T., Fujikawa, T., Miyashita, H., Ikeda, T., Tsukamoto, S., and Nohara, T. (2011). Anti-obesity compounds in green leaves of Eucommia ulmoides. Bioorg. Med. Chem. Lett. *21*, 1786–1791.

Hosoo, S., Koyama, M., Kato, M., Hirata, T., Yamaguchi, Y., Yamasaki, H., Wada, A., Wada, K., Nishibe, S., and Nakamura, K. (2015). The restorative effects of Eucommia ulmoides oliver leaf extract on vascular function in spontaneously hypertensive rats. Molecules *20*, 21971–21981.

Hotamisligil, G.S. (1999). Mechanisms of TNF-α-induced insulin resistance. Exp. Clin. Endocrinol. Diabetes *107*, 119–125.

Hoyt, C.L., Burnette, J.L., and Auster-Gussman, L. (2014). "Obesity is a disease": examining the self-regulatory impact of this public-health message. Psychol. Sci. *25*, 997–1002.

Hsu, H.P., Lai, M.D., Lee, J.C., Yen, M.C., Weng, T.Y., Chen, W.C., Fang, J.H., and Chen, Y.L. (2017). Mucin 2 silencing promotes colon cancer metastasis through interleukin-6 signaling. Sci. Rep. *7*, 5823.

Kimura, I., Ozawa, K., Inoue, D., Imamura, T., Kimura, K., Maeda, T., Terasawa, K., Kashihara, D., Hirano, K., Tani, T., et al. (2013). The gut microbiota suppresses insulin-mediated fat accumulation via the short-chain fatty acid receptor GPR43. Nat. Commun. *4*, 1829.

Kitahara, C.M., Flint, A.J., Gonzalez, A.B., Bernstein, L., Brotzman, M., MacInnis, R.J., Moore, S.C., Robien, K., Rosenberg, P.S., Singh, P.N., et al. (2014). Association between class III obesity (bmi of 40–59 kg/m2) and mortality: a pooled analysis of 20 prospective studies. PLoS Med. *11*, e1001673.

Lee, J.W., Na, D., Park, J.M., Lee, J., Choi, S., and Lee, S.Y. (2012). Systems metabolic engineering of microorganisms for natural and non-natural chemicals. Nat. Chem. Biol. *8*, 536–546.

Mills, E.L., Pierce, K.A., Jedrychowski, M.P., Garrity, R., Winther, S., Vidoni, S., Yoneshiro, T., Spinelli, J.B., Lu, G.Z., Kazak, L., et al. (2018). Accumulation of succinate controls activation of adipose tissue thermogenesis. Nature *560*, 102–106.

Monk, J.M., Wu, W., Lepp, D., Wellings, H.R., Hutchinson, A.L., Liddle, D.M., Graf, D., Pauls, K.P., Robinson, L.E., and Power, K.A. (2019). Navy bean supplemented high-fat diet improves intestinal health, epithelial barrier integrity and critical aspects of the obese inflammatory phenotype. J. Nutr. Biochem. *70*, 91–104.

Nauck, M.A., Vardarli, I., Deacon, C.F., Holst, J.J., and Meier, J.J. (2011). Secretion of glucagon-like peptide-1 (GLP-1) in type 2 diabetes: what is up, what is down? Diabetologia *54*, 10–18.

Osborn, O., and Olefsky, J.M. (2012). The cellular and signaling networks linking the immune system and metabolism in disease. Nat. Med. *18*, 363–374.

Reimer, R.A., Darimont, C., Gremlich, S., Nicolas-Métral, V., Rüegg, U.T., and Macé, K. (2001). A human cellular model for studying the regulation of glucagon-like peptide-1 secretion. Endocrinology *142*, 4522–4528.

Ridaura, V.K., Faith, J.J., Rey, F.E., Cheng, J., Duncan, A.E., Kau, A.L., Griffin, N.W., Lombard, V., Henrissat, B., Bain, J.R., et al. (2013). Gut microbiota from twins discordant for obesity modulate metabolism in mice. Science *341*, 1241214.

Sato, J., Kanazawa, A., Ikeda, F., Yoshihara, T., Goto, H., Abe, H., Komiya, K., Kawaguchi, M., Shimizu, T., Ogihara, T., et al. (2014). Gut dysbiosis and detection of "live gut bacteria" in blood of Japanese patients with type 2 diabetes. Diabetes Care *37*, 2343–2350.

De Vadder, F., Kovatcheva-Datchary, P., Zitoun, C., Duchampt, A., Bäckhed, F., and Mithieux, G. (2016). Microbiota-produced succinate improves glucose homeostasis via intestinal gluconeogenesis. Cell Metab. *24*, 151–157.

Velcich, A., Yang, W.C., Heyer, J., Fragale, A., Nicholas, C., Viani, S., Kucherlapati, R., Lipkin, M., Yang, K., and Augenlicht, L. (2002). Colorectal cancer in mice genetically deficient in the mucin Muc2. Science *295*, 1726–1729.

Wang, K., Liao, M., Zhou, N., Bao, L., Ma, K., Zheng, Z., Wang, Y., Liu, C., Wang, W., Wang, J., et al. (2019). Parabacteroides distasonis alleviates obesity and metabolic dysfunctions via production of succinate and secondary bile acids. Cell Rep. *26*, 222–235.e5.

iScience, Volume *23*

Supplemental Information

Asperuloside Improves Obesity and Type 2 Diabetes through Modulation of Gut Microbiota and Metabolic Signaling

Anna Nakamura, Yoko Yokoyama, Kazuki Tanaka, Giorgia Benegiamo, Akiyoshi Hirayama, Qi Zhu, Naho Kitamura, Taichi Sugizaki, Kohkichi Morimoto, Hiroshi Itoh, Shinji Fukuda, Johan Auwerx, Kazuo Tsubota, and Mitsuhiro Watanabe

Transparent Methods

Materials

Asperuloside (ASP) was obtained from KOBAYASHI Pharmaceutical Co., Ltd. Japan.

Animal Studies

All animal experiments were performed in accordance with the standards set forth in the Guidelines for the Use and Care of Laboratory Animals at Keio University, Japan. The protocols were approved by the Institute for Experimental Animals of Keio University. Male C57BL/6J mice of 5 weeks of age, were obtained from Japan SLC, Inc. All mice were maintained in a temperature-controlled (23℃) facility with a 12-h light/dark cycle and were given free access to food and water. The mice were placed on the test diet after one-week acclimation. The control diet and high fat diet were obtained from Research Diets, Inc. The control diet (D12450B) contained 20kcal% protein, 70kcal% carbohydrate, and 10kcal% fat, and the high fat diet (D12492) contained 20kcal% protein, 20kcal% carbohydrate, and 60kcal% fat. For treatment with ASP, mice were fed high fat diets with 0.25% (w/w) ASP. The mice were fasted 6-h before harvesting blood for subsequent blood measurements and tissues for RNA isolation and histology.

mRNA Expression Analysis by Quantitative RT-PCR

Total RNA was extracted from tissue samples using the RNeasy Mini Kit (QIAGEN, Hilden, Germany). The cDNA was synthesized from total RNA with the Prime Script RT Reagent Kit (Takara Bio Inc., Shiga, Japan). The expression levels were analyzed in cDNA synthesized from total mRNA using real time PCR. The sequences of the primer sets used are displayed in Supplemental Table 1.

Oral glucose tolerance test (OGTT) and intraperitoneal insulin tolerance test (IPITT)

The OGTT was performed in animals that were fasted 6-h. Glucose (Otsuka pharmaceutical factory Inc., Tokushima, Japan) was administered by gavage at a dose of 2 g/kg. An IPITT was done in 6-h fasted animals. Insulin (Humalin N, Eli Lilly Japan, Kobe, Japan) was injected at a dose of 0.75 units/kg. Glucose quantification was done with the GUNZE Life check (GUNZE Limited, Osaka, Japan).

Plasma measurements

Lipid composition, plasma total cholesterol and NEFA were determined by enzymatic assay kits from Labo Assay TM series (FUJIFILM Wako Pure Chemical Corporation, Osaka, Japan). TG were measured by determiner L TG-Ⅱ (Hitachi Chemical Diagnostics System Co., Ltd., Chuo-ku, Tokyo). TNFα was quantified by Quantikine ELISA Kit (R&D Systems, MN, USA). MCP-1 was measured by MCP-1 ELIZA kit (Thermo Fisher Scientific, MA, USA). The level of the plasma lipopolysaccharide (LPS) was determined by ELISA Kit for Lipopolysaccharide (LPS) (Cloud-Clone Corp., TX, USA) according to the operating instructions.

Metabolite Extraction and CE-TOFMS-based Metabolome Analysis

Cecal contents were used for metabolite extraction as described previously with slight modification (Ishii et al., 2018). Briefly, 10 mg of freeze-dried cecal contents were suspended in 500μL of methanol supplemented with the internal standards (20μM each of methionine sulfone and D-camphor-10-sulfonic acid (CSA)). The mixture was shaken vigorously with three 3-mm beads and 100mg of 0.1-mm zirconia beads (BioSpec Products, Inc., OK, USA) by ShakeMaster® NEO (Biomedical Science, Tokyo, Japan). After extraction of cecal metabolites by standard chloroform-methanol extraction method, the aqueous phase was centrifuged at 4600 × g for 15min at 20℃, and the supernatant was transferred to a 5-kDa-cutoff filter column (Ultrafree MC-PHHCC 250 / pk for Metabolome Analysis, (Human Metabolome Technologies, Tsuruoka, Japan) and centrifuged at 9100 × g for 3 - 7h at 4℃. The filtrate sample was dried under vacuum and the residue then was dissolved in 40 μ of Milli-Q water containing reference compounds (200 μ M each of 3-aminopyrrolidine and time state). The level of extracted metabolites were measured in both positive and negative modes using CE-TOFMS as described previously (Sugimoto et al., 2010). All CE-TOFMS experiments were performed using an Agilent capillary electrophoresis system (Agilent Technologies, CA, USA). Annotation tables were produced from measurement of standard compounds and were aligned with the datasets according to similar m/z value and normalized migration time. Then, peak areas were normalized against those of the internal standards methionine sulfone and CSA for cationic and anionic metabolites, respectively. Concentrations of each metabolite were calculated based on their relative peak areas and concentrations of standard compounds. The statistical analysis was performed using online tool Metaboanalyst (Xia and Wishart, 2011).

DNA Extraction

DNA from cecal contents was extracted following methods as described previously (Furusawa et al., 2013). In brief, cecal content samples were initially freeze dried by using VD-800R lyophilizer (TAITEC, Saitama, Japan) for at least 12 hours. Samples were disrupted with 3-mm Zirconia Beads by vigorous shaking (1,500rpm, for 10 min) using Shake Master (Biomedical Science, Tokyo, Japan). About 10 mg cecal contents were suspended with DNA extraction buffer containing 200 μL of 10% (w/v) SDS/TE (10 mM Tris-HCl, 1 mM EDTA, and pH 8.0) solution, 400 μL of phenol/chloroform/isoamyl alcohol (25 : 24 : 1), and 200 μL of 3 M sodium acetate. Obtained emulsions were further disrupted with 0.1 mm zirconia/silica beads by vigorous shaking (1,500 rpm. for 5 min) using Shake Master. After centrifugation at 17,800 ×g for 5 min at 20℃, bacterial genomic DNA was purified by the standard phenol/chloroform/isoamyl alcohol protocol. RNAs in the sample were removed by RNase A treatment, and then DNA samples were purified again by the standard phenol/chloroform/isoamyl alcohol treatment.

Microbiome analysis by 16S rRNA gene sequencing

Genomic DNAs extraction was performed previously with some modifications (Ishii et al., 2018). 16S rRNA genes in the fecal DNA samples were analyzed using a MiSeq sequencer (Illumina, CA, USA). The V1-V2 region of the 16S rRNA genes was amplified from the DNA isolated from cecal contents using bacterial universal primer set 27Fmod (5′ -AGRGTTTGATYMTGGCTCAG-3′) and 338R (5′ -TGCTGCCTCCCGTAGGAGT-3′). PCR was performed with Tks Gflex DNA Polymerase (Takara Bio Inc., Shiga, Japan) and amplified according the following program: one denaturation step at 98°C for 1 min, followed by 20 cycles of 98°C for 10 s, 55°C for 15 s, and 68°C for 30 s, and a final extension step at 68°C for 3 min. The amplified products were purified using Agencourt AMPure XP (Beckman Coulter) and then further amplified using forward primer (5′ -AATGATACGGCGACCACCGAGATCTACAC- NNN NNNNN-TATGGTAATTGT-AGRGTTTGATYMTGGCTCAG-3′) containing the P5 sequence, a unique 8 bp barcode sequence for each sample (indicated in N), Rd1 SP sequence and 27Fmod primer and reverse primer (5′ -CAAGCAGAAGACGGCATACGAGAT-NNNNNNNN-AGTCAGTCAGCC- TGC TGCCTCCCGAGGAGT-3′) containing the P7 sequence, a unique 8-bp barcode sequence for each sample (indicated by strings of Ns), Rd2 SP sequence, and 338R primer. After purification using Agencourt AMPure XP, mixed sample was prepared by pooling approximately equal amounts of PCR amplicons from each sample. Finally, MiSeq sequencing was performed according to the manufacturer's instructions. In this study, 2 × 300 bp paired-end sequencing was employed.

Microbiome Data Analysis Using QIIME

First, to assemble the paired end reads, fast length adjustment of short reads (FLASH) (v1.2.11) (Magoc and Salzberg, 2011) was used. Assembled reads with an average -value < 25 were filtered out using in-house script. 5,000 filter-passed reads were randomly selected from each sample and used for further analysis. Reads were then processed using quantitative insights into microbial ecology (QIIME) (v1.8.0) pipeline (Caporaso et al., 2010). Sequences were clustered into operational taxonomic units (OTUs) using 97% sequence similarity and OTUs were assigned to taxonomy using RDP classifier.

Sequence accession number

The microbiome analysis data have been deposited at the DDBJ Sequence Read Archive (http://trace.ddbj.nig.ac.jp/dra/) under accession number DRA009825.

Histology and quantification of the adipocyte.

Adipose tissues were harvested and immediately fixed Tissue-Tek UFIX (Sakura Finetek Japan, Tokyo, Japan). Hematoxylin and eosin (H&E) staining was conducted using paraffin-embedded tissue sections. The adipocyte diameter was quantified by using ImageJ software (NIH, MD, USA) (Schneider et al. 2012).

Cell culture

In vitro experiments were performed with NCI-H716 cells in RPMI1640 medium with 10% FBS with vehicle (DMSO), TCA, or ASP at the indicated concentrations. Measurement of GLP-1 release was measured in cultural medium after treatments with the chemical compounds, with supernatants of the medium containing a protease inhibitor cocktail (Roche Diagnostics K.K., Tokyo, Japan). GLP-1 concentration was measured using the GLP-1 Active Assay Kit from IBL (IBL Co., Gunma, Japan). The GLP-1 concentrations were normalized against total cell amounts measured by TaKaRa BCA protein Assay Kit (Takara Bio Inc., Shiga, Japan).

Statistical analysis

Values were reported as mean ± SEM. Statistical differences were determined by either one-way ANOVA or Student's t test with using Graph Pad Prism 8. Statistical significance is displayed as follows: *$p < 0.05$, **$p < 0.01$, ***$p < 0.001$ HFD vs HFD-Asp, #$p < 0.05$, ##$p < 0.01$, ###$p < 0.001$ HFD vs Control, +$p < 0.05$, ++$p < 0.01$, +++$p < 0.001$ Control vs HFD-Asp.

References

Caporaso, J.G., Kuczynski, J., Stombaugh, J., Bittinger, K., Bushman, F.D., Costello, E.K., Fierer, N., Peña, A.G., Goodrich, J.K., Gordon, J.I., et al. (2010). QIIME allows analysis of high-throughput community sequencing data. Nat. Methods 7, 335–336.

Ishii, C., Nakanishi, Y., Murakami, S., Nozu, R., Ueno, M., Hioki, K., Aw, W., Hirayama, A., Soga, T., Ito, M., et al. (2018). A Metabologenomic Approach Reveals Changes in the Intestinal Environment of Mice Fed on American Diet. Int. J. Mol. Sci. 19, 4079.

Sugimoto, M., Wong, D.T., Hirayama, A., Soga, T., and Tomita, M. (2010). Capillary electrophoresis mass spectrometry-based saliva metabolomics identified oral, breast and pancreatic cancer-specific profiles. Metabolomics 6, 78–95.

Schneider, C.A., Rasband, W.S., Eliceiri, K.W. (2012). NIH Image to ImageJ: 25 years of image analysis. Nat. Methods 9, 671-675.

Xia, J., and Wishart, D.S. (2011). Web-based inference of biological patterns, functions and pathways from metabolomic data using MetaboAnalyst. Nat. Protoc. 6, 743–760.

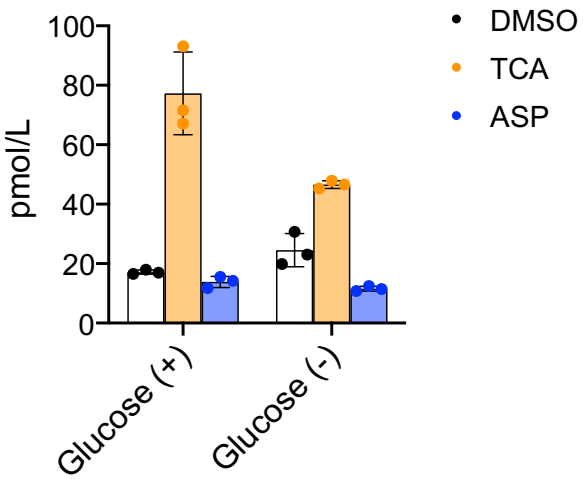

Figure S1. Related to Figure 1. Asperuloside (ASP) stimulates GLP-1 secretion indirectly. GLP-1 concentration secreted from NCI-H716 cell line cultured for 30 minutes in the absence or presence of glucose and either treated with DMSO (vehicle), taurocholic acid (100μM), or ASP (100μM) added within the medium.

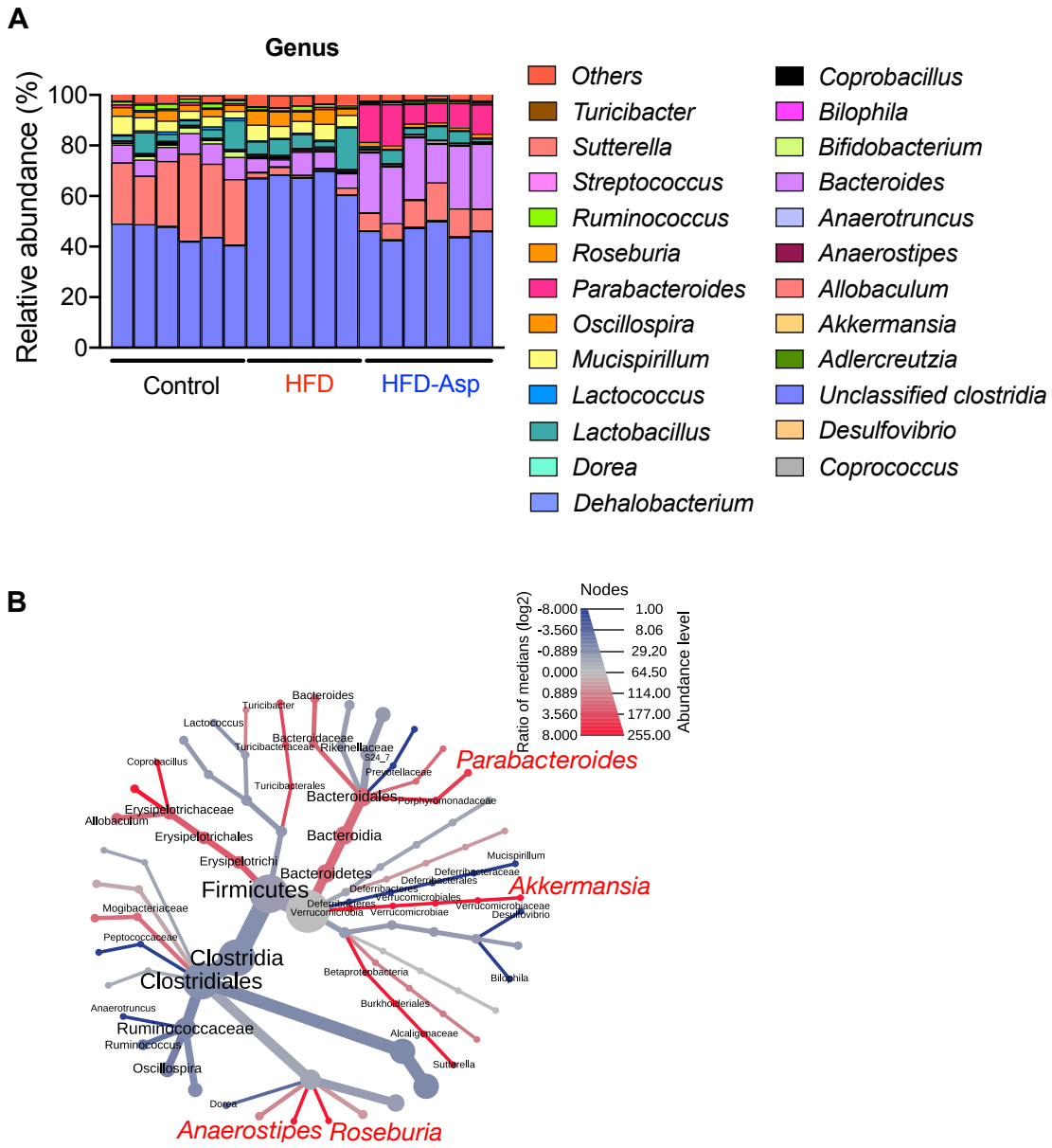

Figure S2. Related to Figure 2. ASP changes gut microbiota community and increases specific bacteria in genus level. Analysis of 16s rRNA gene sequences on the mice used in Figure 1. (A) Genus level taxonomic distributions of the microbial communities in cecal contents of mice fed with the 3 different diets. (B) Bacterial community structure at genus level represented with a heat tree compared high-fat diet (HFD) fed mice and HFD +0.25% asperuloside fed mice.

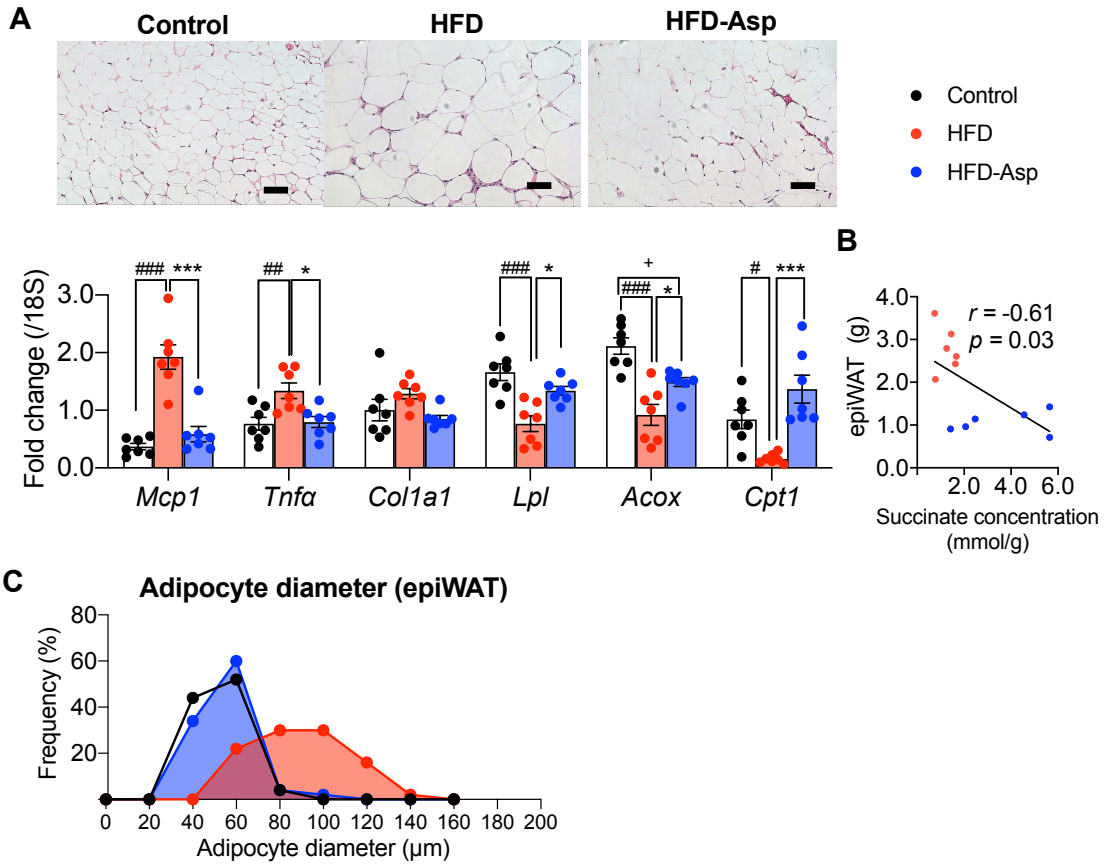

Figure S3. Related to Figure 4. ASP changes adipocyte metabolism. Analysis on the mice used in Figure 1. (A) Histological analysis and expression of mRNA levels of selected genes qPCR analysis in the epididymal white adipose tissue (epiWAT). Adipocyte morphology was assessed by H&E staining (Scale bar: 50μm). (B) Correlation analysis between succinate concentration and epiWAT weight. Y axis: weight of epiWAT, X axis: succinate concentration of cecal contents. (C) Adipocyte diameter. Results are expressed as mean ± SEM (n = 6-7 mice for each group). *p < 0.05, **p < 0.01, ***p < 0.001 HFD vs HFD-Asp, #p < 0.05, ##p < 0.01, ###p < 0.001 HFD vs Control, +p < 0.05, ++p < 0.01, +++p < 0.001 Control vs HFD-Asp. Statistical analysis with one-way ANOVA followed Tukey's multiple comparison test.

Table S1. Related to Figure 4. Primer sequences.

Gene	Forward primer (5'→3')	Reverse primer (5'→3')
18S	TTCTGGCCAACGGTCTAGACAAC	CCAGTGGTCTTGGTGTGCTGA
Acox	TTCTACCAATCTGGCTGCAC	GTGGGTGGTATGGTGTCGTA
Col1a1	CAACCTGGACGCCATCAAG	CGTGGAATCTTCCGGCTGTAG
Cpt1	TCATTGGCCACCAGTTCCATTA	CCAATGGCTGCCACACTCTC
Dio2	TTCTGAGCCGCTCCAAGT	GGAGCATCTTCACCCAGTTT
Defa	GGTGATCATCAGACCCCAGCATCAGT	AAGAGACTAAAACTGAGGAGCAGC
Lpl	CAGCAGGGAGTCAATGAAGA	ATCCGTGTGATTGCAGAGAG
Mcp1	CTGGATCGGAACCAAATGAG	CGGGTCAACTTCACATTCAA
Muc2	GGGAGGGTGGAAGTGGCATTGT	TGCTGGGGTTTTTGTGAATCTC
Muc3	AACTGCAGCTACGGCAAATGTC	AGGTTTCGCCTACCATCGTAAC
Pgc1α	AAGGGCCAAACAGAGAGAGA	GCGTTGTGTCAGGTCTGATT
Pla2g2	AGGATTCCCCAAGGATGCCAC	CAGCCGTTTCTGACAGGAGTTCTGG
Pparδ	TCTGCCATCTTCTGCAGCAGCTT	CTCTTCATCGCGGCCATCATTCT
Prdm16	CAGCACGGTGAAGCCATTC	GCGTGCATCCGCTTGTG
Reg3γ	CTGGGACAGTGACCTGGACT	GCACCTCAGGGAAGAGTCTG
Tnfα	CTGGGACAGTGACCTGGACT	GCACCTCAGGGAAGAGTCTG
Tjp1	GACCAATAGCTGATGTTGCCAGAG	TATGAAGGCGAATGATGCCAGA
Tjp2	GACATCTATGCGGTTCCAATCAA	TGGTGTCCTGGTAAAGTCTGGAAG
Ucp1	GGCCCTTGTAAACAACAAAATAC	GGCAACAAGAGCTGACAGTAAAT
Ucp2	AGAAGTGAAGTGGCAAGGGA	GCTGAGCTGGTGACCTATGA